Optical signatures of strain-induced ferromagnetism in a $LaCoO_3$ thin film

F. Abadizaman,[1] D. Munzar,[1] M. Kiaba,[1] and A. Dubroka[1,2,*]

[1]*Department of Condensed Matter Physics, Faculty of Science, Masaryk University, Kotlářská 2, 611 37 Brno, Czech Republic*

[2]*Central European Institute of Technology, Brno University of Technology, 612 00 Brno, Czech Republic*

(Received 16 April 2024; revised 27 November 2024; accepted 4 December 2024; published 24 December 2024)

Using spectroscopic ellipsometry, we studied the optical conductivity of $LaCoO_3$ with various degrees of strain. The optical response of the compressively strained $LaCoO_3$ film is qualitatively similar to the one of the unstrained $LaCoO_3$ polycrystalline sample and exhibits a redistribution of the spectral weight between ∼0.2 and 6 eV, which is most likely related to the thermal excitation of the high-spin (HS) states. The optical response of the ferromagnetic (FM) tensile strained film exhibits clear signatures of the FM state. Below the Curie temperature $T_c = 82$ K, a spectral weight transfer sets on from high energies (between 3.3 and 5.6 eV) to low energies (between 0.2 and 3.3 eV). The temperature dependence of the low-energy spectral weight can be understood in the framework of the HS biexciton model of Sotnikov *et al.* [SciPost Phys. **8**, 082 (2020)] as corresponding to the increase of the concentration of the HS states that are stabilized below T_c. The magnitude of the redistribution of the spectral weight due to the formation of the FM state is sizable and corresponds to 0.009 e per Co ion. We discuss it in terms of the effective kinetic energy of Co 3d bands.

DOI: 10.1103/PhysRevB.110.235151

I. INTRODUCTION

$LaCoO_3$ has been studied extensively for its unusual magnetic and electronic properties. At low temperatures, <50 K, bulk $LaCoO_3$ exhibits a nonmagnetic insulating behavior with a small optical gap of ∼0.2 eV [1,2]. In an intermediate temperature range of ∼50–400 K, it exhibits paramagnetic properties while preserving the insulator behavior with a reduced resistance compared with the low-temperature values [1]. At temperatures >500 K, the insulator-to-metal transition occurs [1]. The magnetic properties of $LaCoO_3$ can be altered by strain. It was observed that the tensile strain induces ferromagnetic (FM) order, while $LaCoO_3$ remains insulating [3]. The microscopic mechanism of this FM state is likely qualitatively different from the double-exchange mechanism of the FM state occurring in conducting doped cobaltites [4,5], and its nature is a topic of an ongoing debate [6–10].

The unusual electronic and magnetic properties of bulk $LaCoO_3$ are caused by the specific electronic structure where several spin states are nearly degenerate. It is generally accepted that the unusual behavior in the intermediate temperature range is caused by thermal excitation of higher spin states compared with the low-temperature low-spin (LS) ground state, with the Co electronic configuration t_{2g}^6. There has been a long debate over which spin states are excited at higher temperatures, whether these are dominantly intermediate-spin (IS) states, $t_{2g}^5 e_g^1$, or high-spin (HS) states, $t_{2g}^4 e_g^2$ [11–20]. This debate was recently advanced by authors of a joint theoretical and experimental work reporting a pronounced dispersion of IS excitations [21–23]. This led to a model of thermally excited HS excitons viewed as biexcitons consisting of tightly bound (on the same Co atom) IS excitons with different orbital character. In this approach, both IS and HS states are essential for understanding the low-energy dynamics of $LaCoO_3$. The energy of the HS biexciton is ∼20 meV at low temperatures, and its energy significantly increases with temperature [23].

The strain-induced FM state in $LaCoO_3$ epitaxial films is usually induced by a substrate with a small lattice mismatch. The Curie temperature (T_c) of $LaCoO_3$ films deposited on (100)-oriented $(LaAlO_3)_{0.3}(Sr_2TaAlO_6)_{0.7}$ (LSAT) or $SrTiO_3$ substrates is ∼80–85 K [8,24–28], and T_c can reach up to 94 K in films deposited on (110)-oriented LSAT substrates [6]. Several aspects potentially important for the mechanism of the FM state were reported. Lattice distortion with propagation vector $(\frac{1}{4}, -\frac{1}{4}, \frac{1}{4})$ was observed [6], an important role of the oxygen vacancies was suggested [7,8], and microscopic inhomogeneities of the FM state were observed [9]. Recently, in the framework of the HS biexciton model [23], it was proposed by Sotnikov *et al.* [10] that the strain-induced FM originates from the interaction between HS states via virtual IS states.

In this paper, we would like to contribute to the discussion about the mechanism of the strain-induced FM state by examining the optical response. We study the optical properties of unstrained $LaCoO_3$ (polycrystalline sample) and tensile and

*Contact author: dubroka@physics.muni.cz

compressively strained $LaCoO_3$ films using ellipsometry in the energy range of the interband transitions between 0.2 and 6.5 eV. Ellipsometry is an established technique that allows the determination of the optical response with a high sensitivity and reproducibility. The temperature-dependent optical response in a wide energy range allows us to map the essential redistributions of optical spectral weight upon different phase transitions, which reflect the underlying changes of the electronic structure [29]. We observed that the compressive strain does not qualitatively change the optical response. In contrast, in the FM tensile strained film, the optical response is significantly altered, and it exhibits clear features due to the formation of the FM state. We determine the energy range of the FM-related redistribution of the spectral weight and quantify its magnitude.

II. EXPERIMENT

In this paper, $LaCoO_3$ samples with different degrees of strain were studied: polycrystalline $LaCoO_3$ (no strain), $LaCoO_3$ thin film deposited on $LaAlO_3$ substrate (compressive strain), and $LaCoO_3$ thin film deposited on LSAT substrate (tensile strain). The thin films were grown using pulsed laser deposition and annealed *in situ* at the deposition temperature of 650 °C under 10 Torr oxygen pressure to decrease the oxygen vacancy concentration [30]. The lateral dimension of thin films is 10×10 mm^2, and the thickness of the films was determined using x-ray reflectivity (Rigaku Smartlab) to be ∼22 nm. The measurements of the magnetic moment were performed using a vibrating sample magnetometer (Quantum Design Versalab).

Ellipsometry measurements were performed on the thin films and the bare substrates with a Woollam VASE ellipsometer (0.6–6.5 eV) and Woollam IR-VASE ellipsometer (0.1–0.6 eV) in the temperature range from 300 to 7 K using a custom designed ultrahigh vacuum closed-cycle He cryostat (Cold Edge). The cryostat is equipped with an ultralow vibration interface, ensuring that no vibrations influence the measurements. Copper gasket-sealed fused-silica windows were used in the range covered with the VASE ellipsometer. The window polarization effects were corrected. The base pressure in the sample chamber was 3×10^{-8} mbar at room temperature and about an order of magnitude lower at 7 K. A custom-designed second cold shield improved the local vacuum near the sample through the cryopumping effect. We have verified that no traces of ice formation on the sample are found in the spectra at any temperature. In the midinfrared range covered with the IR-VASE ellipsometer, the KBr windows sealed with a Viton O-ring were used. KBr has negligible polarization influence on the beam. A minor vacuum degradation to 7×10^{-8} mbar at 300 K due to the O-ring sealing is acceptable for the long wavelengths of the midinfrared range, and we confirmed that no traces of ice formation were found in the spectra. All measurements were repeated several times and were found reproducible. The optical constants of the thin film were obtained at each measured energy from the ellipsometric angles Ψ and Δ using the standard model of coherent interferences in a thin film on a substrate [31] without the involvement of the Kramers-Kronig relations.

TABLE I. Lattice parameters of samples determined by x-ray diffraction. For the bulk samples (polycrystalline $LaCoO_3$ and the substrates), the lattice parameter corresponds to the bulk pseudocubic lattice constant, whereas for the films, it denotes the out-of-plane lattice constant.

Sample	Lattice constant (Å)	$\varepsilon_\perp$ (%)	$\varepsilon_\parallel$ (%)
Polycrystalline $LaCoO_3$	3.825		
$LaAlO_3$ substrate	3.787		
LSAT substrate	3.866		
$LaCoO_3/LaAlO_3$ film	3.853	0.73	−0.99
$LaCoO_3$/LSAT film	3.792	−0.86	1.07

III. DATA ANALYSIS AND DISCUSSION

We have probed the structural properties of our films using x-ray diffraction. The reciprocal space maps of the $LaCoO_3$ film deposited on LSAT substrate ($LaCoO_3$/LSAT) measured near the symmetrical (004) diffraction and near the asymmetrical (103) diffraction are shown in Figs. 1(a) and 1(b), respectively. Analogous maps for the $LaCoO_3$ film deposited on $LaAlO_3$ substrate ($LaCoO_3/LaAlO_3$) are shown in Figs. 1(c) and 1(d). They exhibit strong maxima due to the substrate diffraction and distinct maxima due to the $LaCoO_3$ diffraction at the same Q_x values, depicting that the films are epitaxial and fully strained. The lattice parameters of the samples were determined from the positions of the $LaCoO_3$ diffractions, and the results are shown in Table I, including the in-plane and out-of-plane values of film strain obtained from the lattice constants. The $LaCoO_3$/LSAT film has a tensile strain of 1.07%, whereas the $LaCoO_3/LaAlO_3$ film exhibits a compressive strain of −0.99%.

Figure 1(e) shows the temperature dependence of magnetization of all samples measured in a magnetic field of 10 mT parallel to their surface. The $LaCoO_3$/LSAT film exhibits an onset of FM with T_c of ∼82 K, whereas the other samples are nonmagnetic in the measured temperature range. The value of the saturated magnetic moment of the $LaCoO_3$/LSAT film at 50 K is obtained from the hysteresis loop shown in Fig. 1(f) and amounts to $\mu_s = 0.5\ \mu_B$/Co, which is in a good agreement with Refs. [27,28].

An overview of the optical data is presented in Fig. 2. The left, middle, and right columns correspond to the $LaCoO_3$ polycrystal, $LaCoO_3/LaAlO_3$ film, and $LaCoO_3$/LSAT film, respectively. The top row presents the real part of the optical conductivity σ_1 as a function of energy E of the incident photons. Overall, the spectra of all samples have similar shapes. They exhibit an optical gap of 0.2–0.3 eV and several absorption bands that we label as $\alpha, \beta, \gamma, \delta$, and ε, see Fig. 2(a). The energies of the bands α, β, and γ agree very well with those found in Ref. [2]. The band structure calculations suggest that the bands α and β are due to Co $t_{2g} \rightarrow t_{2g}$ and Co $t_{2g} \rightarrow e_g$ transitions, respectively [2]. Based on the calculated orbital resolved density of states (see Fig. 2 in Ref. [2]), we further suggest that (i) the band γ is also due to Co $t_{2g} \rightarrow e_g$ transitions and that (ii) the O $2p \rightarrow$ Co e_g transitions give rise to the broad band δ centered at ∼4.3 eV (rather than to the band γ as proposed in Ref. [2]). The absorption band ε likely corresponds to transitions involving La orbitals since

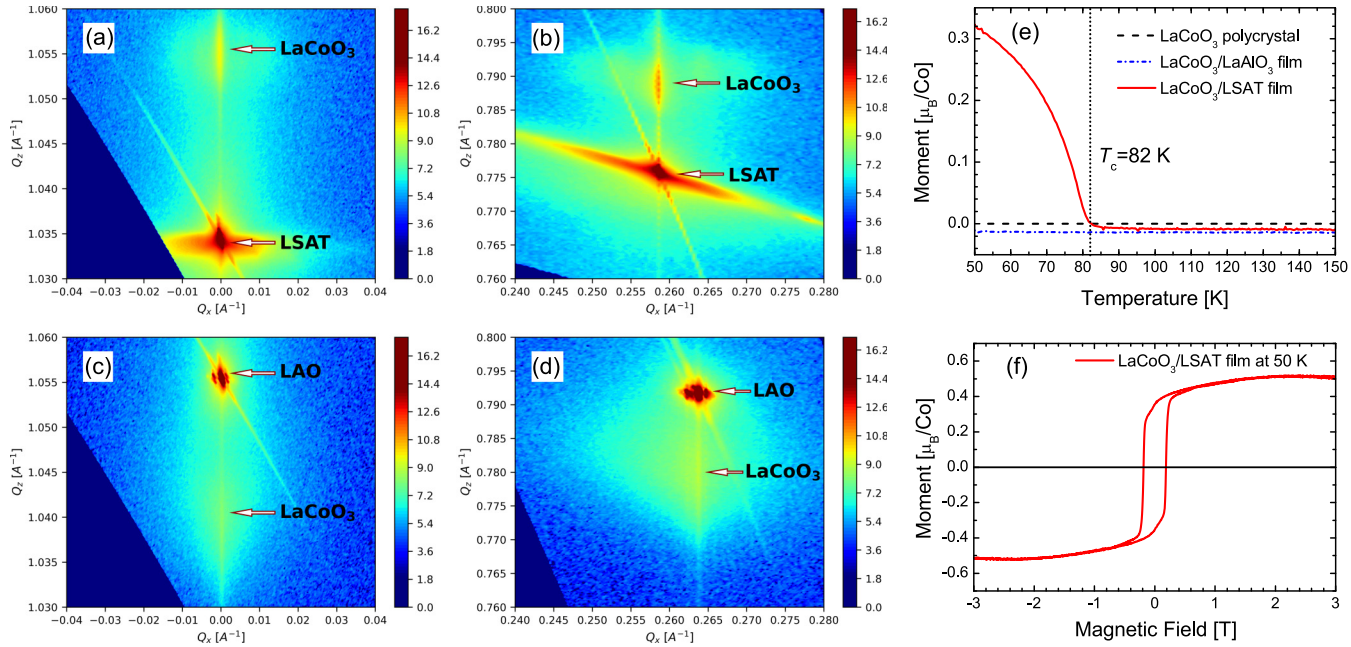

FIG. 1. X-ray reciprocal space maps of $LaCoO_3$ film grown on LSAT substrate (a) near the symmetrical (004) diffraction and (b) near the asymmetrical (103) diffraction. The diffraction peaks due to the substrate and $LaCoO_3$ are denoted by the arrows. (c) and (d) Analogous maps for the $LaCoO_3$ film grown on $LaAlO_3$ (LAO) substrate. (e) Magnetic moment as a function of temperature of the $LaCoO_3$ polycrystalline sample and of the $LaCoO_3/LaAlO_3$ and $LaCoO_3$/LSAT films, measured in a magnetic field of 10 mT. (f) Hysteresis loop of the $LaCoO_3$/LSAT film acquired at 50 K.

its intensity decreases with increasing Sr doping, see Ref. [5]. Another $LaCoO_3$ band structure determined by dynamical mean-field theory can be found in Ref. [32].

The optical data of materials with strongly correlated electrons are often discussed in terms of the effective number of electrons $N_{\mathrm{eff}}(\omega_L, \omega_H)$ per unit cell (or spectral weight) that is a measure of absorption of electromagnetic radiation in an energy interval $(\hbar\omega_L, \hbar\omega_H)$:

$$N_{\mathrm{eff}}(\omega_L, \omega_H) = \frac{2mV}{\pi e^2} \int_{\omega_L}^{\omega_H} \sigma_1(\omega)\, \mathrm{d}\omega. \tag{1}$$

Here, m is the electron mass, V is the volume of the unit cell, and e is the elementary charge [29]. Spectral weight redistributions with changing temperature, which can be described in terms of N_{eff}, are frequently studied because they reflect the underlying changes in the electronic structure. We recall that the common optical sum rule states that the total spectral weight $N_{\mathrm{eff}}(0, \infty)$ is equal to the total number of electrons per unit cell, and consequently, it is independent of temperature [33].

To visualize the redistribution of spectral weight with temperature, the second row of Fig. 2 shows the real parts of the optical conductivities relative to the ones measured at the lowest temperature of 7 K, $\Delta\sigma_1(T) = \sigma_1(T) - \sigma_1(7\ \mathrm{K})$. Figure 2(d) presents $\Delta\sigma_1(T)$ of the $LaCoO_3$ polycrystal. The temperature dependencies of the absorption bands α, β, δ, and ε are noticeable in $\Delta\sigma_1(T)$; the corresponding features are denoted by the arrows. The band γ is exceptional: The spectrum of $\Delta\sigma_1(T)$ reveals that it consists of two bands denoted as γ_1 and γ_2.

In addition, there are several so-called isosbestic energies (energies where the conductivity is essentially temperature independent) that we denote E', E_M, and E_H. The largest changes of the spectral weights with increasing temperature are twofold: a decrease at high energies (between $E_M = 3.4$ eV and $E_H = 6.2$ eV) and an increase at lower energies (between $E_g = 0.2$ eV and $E' = 1.9$ eV). Additionally, there is a less pronounced temperature dependence of the conductivity between E' and E_M. Considering the sum rule, we can describe these findings as a transfer of spectral weight with increasing temperature from high energies (between E_M and E_H) to lower energies (between E_g and E_M). Similar redistribution of optical spectral weight in bulk $LaCoO_3$ was previously observed by Tokura *et al.* [1], who reported that, with increasing temperature, the low-energy (<1.4 eV) spectral weight increases on the expense of spectral weight at higher energies. Note that a similar redistribution of the spectral weight induced by a laser pulse was observed with femtosecond ellipsometry [34]. The crossing point was found to be ∼2.1 eV, close to $E' = 1.9$ eV found in this paper. In the context of the HS biexciton model [23], the observed redistribution of spectral weight is most likely related to thermal excitation of the HS biexcitons and corresponding changes in the occupation of t_{2g} and e_g orbitals.

The relative conductivity of the compressively strained $LaCoO_3/LaAlO_3$ film is shown in Fig. 2(e). Qualitatively, the spectra are like those of the polycrystalline $LaCoO_3$ shown in Fig. 2(d) with slightly different values of the characteristic energies, $E' = 1.7$, $E_M = 3.6$, and $E_H = 5.9$ eV and larger magnitudes. Particularly, the spectra exhibit the same redistribution of spectral weight with increasing temperature from high energies (between E_M and E_H) to lower energies (between E_g and E').

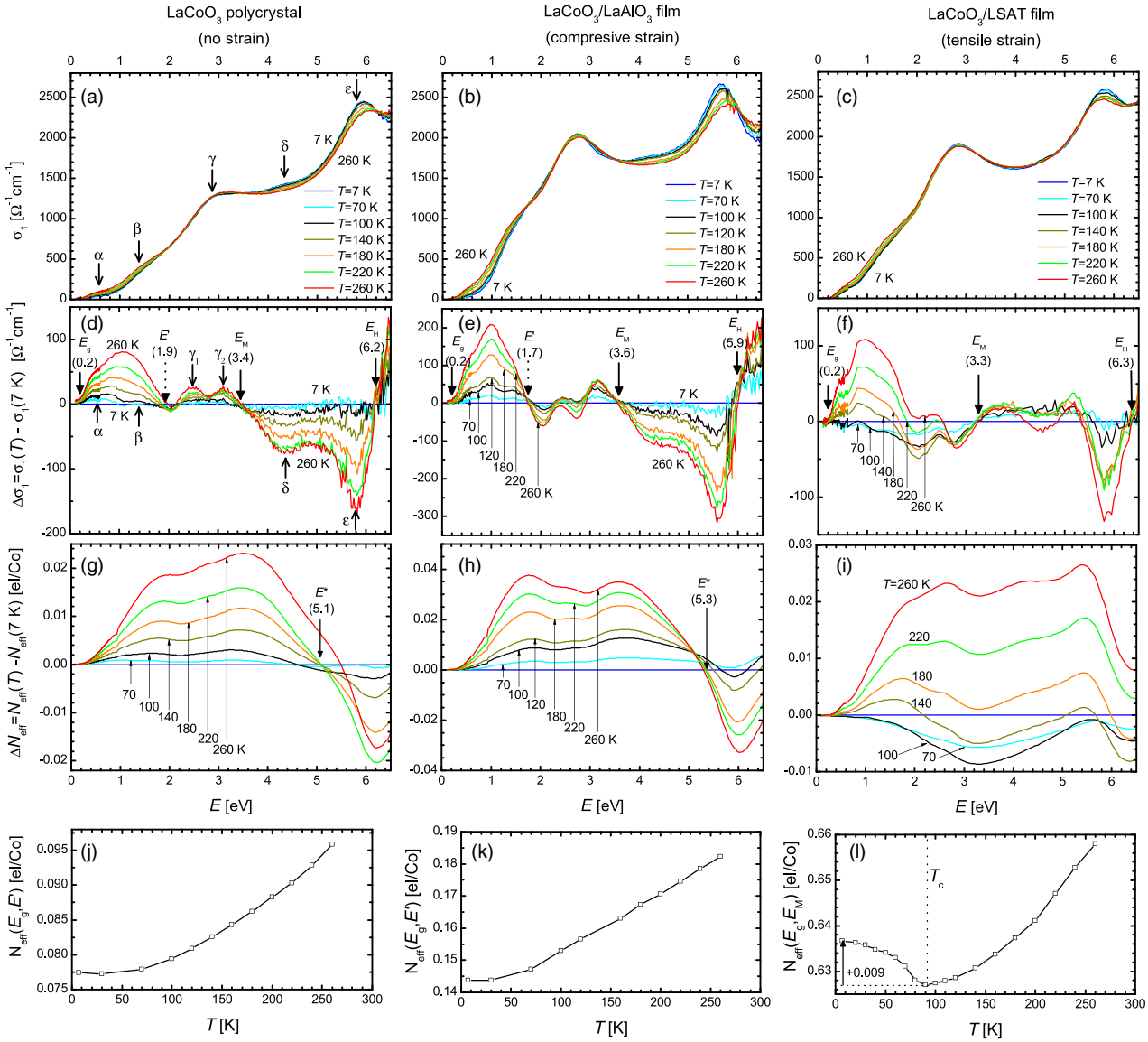

FIG. 2. An overview of the optical data. The left, middle, and right columns correspond to the unstrained $LaCoO_3$ polycrystal, compressively strained $LaCoO_3/LaAlO_3$ thin film, and tensile strained $LaCoO_3$/LSAT film, respectively. The top row (a)–(c) The real part of the optical conductivity $\sigma_1(E,T)$ as a function of energy E and temperature T. The second row (d)–(f) $\Delta\sigma_1 = \sigma_1(T) - \sigma_1(7\text{ K})$. Note that the vertical scale differs from panel to panel. The third row (g)–(i) $\Delta N_{\text{eff}}(E) = N_{\text{eff}}(0.1\text{ eV}, E, T) - N_{\text{eff}}(0.1\text{ eV}, E, T = 7\text{ K})$, as a function of the high energy cutoff E. For definition of N_{eff}, see Eq. (1). (j) and (k) Temperature dependencies of $N_{\text{eff}}(E_g, E')$ and (l) $N_{\text{eff}}(E_g, E_M)$; for definitions of E_g, E', and E_M, see (d)–(f).

The third row of Fig. 2 displays the change of the effective number of electrons as compared with the 7 K data, $\Delta N_{\text{eff}}(E) = N_{\text{eff}}(0.1\text{ eV}, E, T) - N_{\text{eff}}(0.1\text{ eV}, E, T = 7\text{ K})$, as a function of the high-energy cutoff $E = \hbar\omega_H$. The low energy cutoff was chosen to be $\hbar\omega_L = 0.1$ eV, right below the optical gap. The spectral weight due to infrared phonons is thus not considered, but it is negligible compared with the spectral weight of the interband transitions. The energy E^* of the zero crossing of $\Delta N_{\text{eff}}(E)$ corresponds to the energy below which the redistributions of spectral weight are compensated. For the polycrystalline $LaCoO_3$ and for $T = 220$ K, the zero crossing occurs at about $E^* = 5.1$ eV, see Fig. 2(g), and for the compressively strained $LaCoO_3$, it occurs near $E^* = 5.3$ eV, see Fig. 2(h). These values of E^* indicate that the spectral weight of the pronounced dip near 5.8 eV (the band ε) in Figs. 2(d) and 2(e) is compensated by a feature at an energy higher than E_H.

The qualitative similarity between the unstrained polycrystalline $LaCoO_3$ and the compressively strained $LaCoO_3/LaAlO_3$ film can also be seen in the temperature dependence of the low-energy spectral weight $N_{\text{eff}}(E_g, E')$ shown for the $LaCoO_3$ polycrystal in Fig. 2(j) and for the $LaCoO_3/LaAlO_3$ film in Fig. 2(k). Both exhibit a monotonous increase with temperature, which likely corresponds to the thermal population of the HS states. The similarity of the redistribution of the spectral weight between unstrained polycrystalline $LaCoO_3$ and the compressively strained $LaCoO_3/LaAlO_3$ film indicates that the compressive

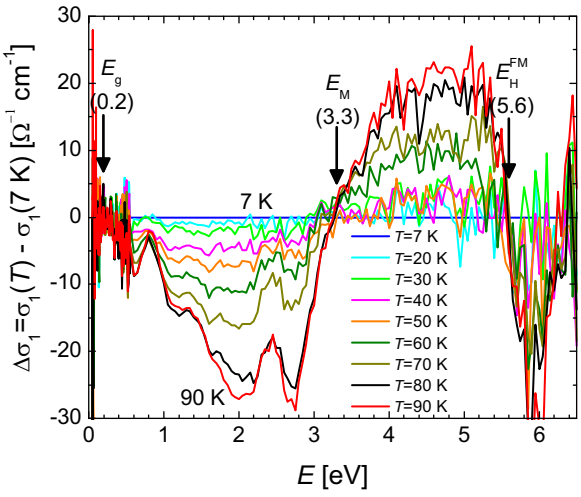

FIG. 3. The real part of the difference optical conductivity $\Delta\sigma_1 = \sigma_1(T) - \sigma_1(7\ \mathrm{K})$ of the ferromagnetic $LaCoO_3$/LSAT film, below and near $T_c = 82$ K.

strain does not induce a qualitative modification of the electronic structure of $LaCoO_3$. The only significant difference is quantitative—the changes with temperature in the compressively strained $LaCoO_3$ are about twice as large as those of the unstrained $LaCoO_3$. This likely corresponds to a lower activation energy of the HS states in the compressively strained $LaCoO_3$ than the unstrained $LaCoO_3$.

Figure 2(f) displays $\Delta\sigma_1$ of the $LaCoO_3$/LSAT film. Apparently, the temperature dependence shows qualitative differences with respect to the previous cases shown in Figs. 2(d) and 2(e). For example, the isosbestic point near the middle of the measured range at $E_M = 3.3$ eV has the opposite signature, i.e., below E_M, the conductivity decreases with increasing temperature in contrast with Fig. 2(d). The origin of the differences becomes clear from the temperature dependence of the low-energy spectral weight $N_{\mathrm{eff}}(E_g, E_M)$ shown in Fig. 2(l), which exhibits a clear onset at T_c with the square root behavior typical for the temperature dependence of an order parameter of a second-order phase transition. The optical response of the $LaCoO_3$/LSAT film exhibits clear signatures of the FM phase transition.

Figure 3 displays in detail $\Delta\sigma_1$ of the $LaCoO_3$/LSAT film below T_c. Since in this temperature range the temperature-dependent changes of nonmagnetic origin are weak, most of the changes correspond to the formation of the FM phase. The spectra exhibit isosbestic points at $E_M = 3.3$ eV and $E_H^{\mathrm{FM}} = 5.6$ eV, as denoted by the arrows. The temperature dependence forms a butterflylike shape with the isosbestic point E_M in the center with two wings with roughly similar areas between $E_g - E_M$ and $E_M - E_H^{\mathrm{FM}}$. The spectral weight is transferred, with increasing temperature, from the low-energy wing into the high-energy wing; therefore, the spectral weight redistribution has the opposite trend as compared with the one observed in the unstrained $LaCoO_3$ and shown in Fig. 2(d). Figure 3 shows that the high-energy limit for the integral shown in Fig. 2(l) was set to track the spectral weight of the low-energy wing and, thus, the FM-induced changes.

Note, however, that the FM-related redistribution of the spectral weight involves significantly different energy scales than those observed in the nonmagnetic samples. In the polycrystalline $LaCoO_3$ and the compressively strained $LaCoO_3/LaAlO_3$ film, the main part of the spectral weight increase at low energies occurs between 0.2 and 1.7–1.9 eV, see Figs. 2(d) and 2(e). In contrast, in the FM $LaCoO_3$/LSAT film, the low-energy wing spans the range between 0.2 and 3.3 eV, with the maximum in the interval between 2 and 2.8 eV, where the conductivity changes in the nonmagnetic samples are only minor. We think that this sizable difference reflects the FM interaction of the HS states that is absent in the nonmagnetic samples. We believe that this sizable change in the involved energy scale is potentially important and should be explained by a theory aiming at a full understanding of the strain-induced FM state in $LaCoO_3$.

Figure 2(l) displays the temperature dependence of the effective number of electrons $N_{\mathrm{eff}}(E_g, E_M)$ corresponding to the low-energy wing. The amount of the spectral weight redistributed due to the formation of the FM state $\Delta N_{\mathrm{eff}}^{\mathrm{FM}}$ can be estimated (as shown by the arrow) as the difference between the value of $N_{\mathrm{eff}}(E_g, E_M)$ at 7 K and that right above T_c. We obtain $\Delta N_{\mathrm{eff}}^{\mathrm{FM}} = +0.009$ elementary charge per Co ion. This estimate neglects the contribution to the temperature dependence of $N_{\mathrm{eff}}(E_g, E_M)$ due to processes unrelated to the FM ordering. We believe that this contribution is small, and if considered, this would slightly increase the obtained value of $\Delta N_{\mathrm{eff}}^{\mathrm{FM}}$.

The value of $\Delta N_{\mathrm{eff}}^{\mathrm{FM}}$ can be estimated as well from $\Delta N_{\mathrm{eff}}(E)$ shown in Fig. 2(i) where, for $T = 100$ K, the value of $\Delta N_{\mathrm{eff}}(E)$ near 3.3 eV yields the value of -0.009. Additionally, $\Delta N_{\mathrm{eff}}(T = 100\ \mathrm{K})$ amounts to -0.001 at $E_H^{\mathrm{FM}} = 5.6$ eV and, thus, almost reaches zero. It indicates that within the accuracy of ~10%, the spectral weight of the high-energy wing compensates for the low-energy wing, and thus, the spectral weight below T_c is essentially conserved below $E_H^{\mathrm{FM}} = 5.6$ eV. In this context, it is interesting to note that, at 260 K, $\Delta N_{\mathrm{eff}}(E)$ does not exhibit any zero crossing in the measured range, and at 6.5 eV, it amounts to a sizable value of 0.008. This demonstrates that, in the tensile strained $LaCoO_3$, the spectral weight redistribution at temperatures above T_c involves transitions at energies above our measurement limit of 6.5 eV.

Next, we discuss possible interpretations of the observed FM-induced transfer of spectral weight $\Delta N_{\mathrm{eff}}^{\mathrm{FM}} = +0.009$. Let us first recall the restricted or tight-binding sum rule [35–38]. Consider the Hubbard model on a cubic lattice with the single-particle tight-binding component of the Hamiltonian involving nearest-neighbor hopping terms only. The effective λ-axis kinetic energy K^{λ}, i.e., the expectation value of the part of the single-particle component containing hopping terms along the λ axis ($\lambda \in \{x, y, z\}$) per unit cell, is connected to the total optical spectral weight:

$$N_{\mathrm{eff}}^{\lambda} = \frac{2mV}{\pi e^2} \int_0^{\infty} \sigma_1^{\lambda}(\omega)\, \mathrm{d}\omega, \tag{2}$$

as follows:

$$K^{\lambda} = -\frac{\hbar^2}{ma_0^2} N_{\text{eff}}^{\lambda}. \tag{3}$$

Here, $\sigma_1^{\lambda}(\omega)$ is the real part of the λ-axis conductivity of the model, and a_0 is the lattice parameter. Equation (3) is the restricted sum rule. Note that, in contrast with the common sum rule mentioned below Eq. (1), N_{eff}^{λ} of Eq. (2) is not temperature independent. The strength of the restricted sum rule in Eq. (3) lies in the fact that it allows one to obtain, at least in principle, the temperature-dependent changes of K^{λ} using optical data; for a relevant example, see Ref. [39]. A transparent proof of Eq. (3) for the case of the two-dimensional (2D) one-band Hubbard model can be found in Sec. IV B 2 of Ref. [38]; extensions to three-dimensional (3D) and multiband Hubbard models are straightforward. For a metal, N_{eff}^{λ} contains the spectral weight of the Drude part of σ^{λ}. For an insulator, both K^{λ} and N_{eff}^{λ} can be expressed as sums over contributions of individual optical transitions (bands), $K^{\lambda} = \sum_n K_n^{\lambda}$, $N_{\text{eff}}^{\lambda} = \sum_n N_{\text{eff},n}^{\lambda}$, and $K_n^{\lambda} = -\frac{\hbar^2}{ma_0^2} N_{\text{eff},n}^{\lambda}$ [40]. For an isotropic system, the total effective kinetic energy $K = K^x + K^y + K^z$ is equal to $3K^{\lambda}$ with λ arbitrary.

In our case, we follow the temperature dependencies of the bands α, β, and γ. As discussed above, these bands likely originate from transitions between Co $3d$ bands. Indeed, the orbital resolved densities of states presented in Ref. [2] suggest that the O $2p \rightarrow$ Co $3d$ transitions have an onset near 3.2 eV and should peak at ∼4 eV, that is, above the low-energy wing of Fig. 3. It is thus meaningful to discuss the temperature dependence of $N_{\text{eff},\alpha}^{x} + N_{\text{eff},\beta}^{x} + N_{\text{eff},\gamma}^{x} \approx N_{\text{eff}}(E_g, E_M)$ in terms of the effective kinetic energy of the Co $3d$ bands K_{3d}. Here, x denotes the axis in the plane of the sample surface accessible by the experiment. Using the formalism outlined above, we obtain the FM-induced change of the effective kinetic energy of the α, β, and γ bands as $\Delta(K_{\alpha}^{x} + K_{\beta}^{x} + K_{\gamma}^{x})_{\text{FM}} = -\frac{\hbar^2}{ma_0^2} \Delta N_{\text{eff}}^{\text{FM}}$, where $\Delta N_{\text{eff}}^{\text{FM}} = \Delta N_{\text{eff}}(E_g, E_M)|_{\text{FM}}$ was determined above. Using further the assumption that the material is essentially optically isotropic and the assumption that the three bands cover most of the spectral weight of Co $3d \rightarrow 3d$ transitions, we obtain $\Delta(K_{3d})_{\text{FM}} = -\frac{3\hbar^2}{ma_0^2} \Delta N_{\text{eff}}^{\text{FM}}$ that amounts to ∼13 meV.

Note that the spectral weight shift is qualitatively the same as in insulating antiferromagnetic $LaMnO_3$ (observed for the electric vector polarized in the direction b with the FM correlations), where the HS absorption band (located at low energies) grows below the ordering temperature on the expense of the LS absorption band (located at higher energies) [39]. It was emphasized in Ref. [40] that the (transition dependent) sum rules provide a unified picture linking the optical and magnetic properties in various materials including manganites [39,41], vanadates [42], and ruthenates [43]. We believe that the same picture applies even in the present case of a strain-induced FM state in insulating cobaltites despite the possible differences in microscopic details of the FM interaction as compared with the other materials.

Note that the direction (or sign) of the observed FM-induced spectral weight redistribution is the same as in the double exchange FM state of metallic cobaltites [5]. In the latter case, similarly, as in metallic FM manganites [44], the FM-induced increase of the Drude peak can be directly assigned to the decrease of the total effective kinetic energy of the conducting electrons [29,38]. For the metallic cobaltites, it was found that the FM-induced reduction of this effective kinetic energy is about twice as large as $k_B T_c$ [5]. Surprisingly, a similar ratio of $\Delta(K_{3d})_{\text{FM}}/k_B T_c$ of ∼2 is observed here for the strain-induced FM in the insulating $LaCoO_3$. Note, however, that in the present case, the effective kinetic energy covers all Co $3d$ bands, including e_g, whereas in the case of the metallic cobaltites, the effective kinetic energy related to the Drude peak corresponds most likely to t_{2g} bands [5]. Since the penetration depth in $LaCoO_3$ in the whole measured range is larger than the thickness of the films (∼22 nm), our optical measurements provide an average response of the films. Our findings, therefore, show that the strain-induced FM state is pronounced and probably occurs in the whole film or at least in a large fraction of the film.

Finally, we briefly discuss the spectral weight redistribution in the context of the model proposed by Sotnikov *et al.* [10]. Provided that the spectral weight of the low-energy wing $N_{\text{eff}}(E_g, E_M)$ is proportional to the population of the HS states, its temperature changes, shown in Fig. 2(l), can be qualitatively understood as follows. Above T_c, the concentration of the HS states is expected to decrease with decreasing temperature as the thermally populated HS states relax into the LS states. Below T_c, the HS states get stabilized by the FM interaction, and thus, their concentration increases with decreasing temperature. An alternative/complementary view uses an argument involving the effective kinetic energy. In the model of Sotnikov *et al.* [10], the FM order originates from a superexchange-type interaction between two immobile HS biexcitons via virtual mobile IS states. The FM ordering of the HS states located at the diagonal positions allows them to fluctuate between two relevant configurations (see Fig. 2(e) in Ref. [10]), which leads to a lowering of their kinetic energy. We speculate that the latter effect yields the observed reduction of the effective kinetic energy of the $3d$ bands whose magnitude is expressed by $\Delta(K_{3d})_{\text{FM}}$.

IV. SUMMARY

Using spectroscopic ellipsometry, we have measured the optical conductivity of $LaCoO_3$ with various degrees of strain. The optical response of the compressively strained $LaCoO_3$ film grown on $LaAlO_3$ substrate is qualitatively similar to that of the unstrained $LaCoO_3$ polycrystalline sample. With increasing temperature, they both exhibit a transfer of spectral weight from high energies (3.5–6 eV) to lower energies (0.2–1.9 eV). This redistribution of spectral weight is most likely related to the thermal excitation of the HS states.

The optical response of the FM tensile strained $LaCoO_3$/LSAT film exhibits clear signatures of the FM state. Below the Curie temperature $T_c = 82$ K, the spectral weight is transferred with increasing temperature from low energies (0.2–3.3 eV) to high energies (3.3–5.6 eV). The temperature dependence of the low-energy spectral weight (0.2–3.3 eV) can be understood in the framework of the HS biexciton model as being due to an increase of the concentration of the HS states below T_c. The amount of spectral weight redistributed due to the formation of the FM

state is sizable and amounts to 0.009 elementary charge per Co ion. It corresponds to the decrease of the effective kinetic energy of the Co 3*d* bands by 13 meV.

ACKNOWLEDGMENTS

We thank O. Caha, J. Chaloupka, A. Hariki, J. Kuneš, and A. Sotnikov for fruitful discussions. We acknowledge the usage of data measured by P. Friš. We acknowledge the financial support by the project Quantum Materials for Applications in Sustainable Technologies Grant No. CZ.02.01.01/00/22_008/0004572, by the Czech Science Foundation under Project No. GA20-10377S and Czech-NanoLab Project No. LM2023051 funded by MEYS CR for the financial support of the measurements/sample fabrication at CEITEC Nano Research Infrastructure.

[1] Y. Tokura, Y. Okimoto, S. Yamaguchi, H. Taniguchi, T. Kimura, and H. Takagi, Thermally induced insulator-metal transition in $LaCoO_3$: A view based on the Mott transition, Phys. Rev. B **58**, R1699 (1998).

[2] D. W. Jeong, W. S. Choi, S. Okamoto, J.-Y. Kim, K. W. Kim, S. J. Moon, D.-Y. Cho, H. N. Lee, and T. W. Noh, Dimensionality control of *d*-orbital occupation in oxide superlattices, Sci. Rep. **4**, 6124 (2014).

[3] D. Fuchs, C. Pinta, T. Schwarz, P. Schweiss, P. Nagel, S. Schuppler, R. Schneider, M. Merz, G. Roth, and H. v. Löhneysen, Ferromagnetic order in epitaxially strained $LaCoO_3$ thin films, Phys. Rev. B **75**, 144402 (2007).

[4] D. Fuchs, M. Merz, P. Nagel, R. Schneider, S. Schuppler, and H. von Löhneysen, Double exchange via t_{2g} orbitals and the Jahn-Teller effect in ferromagnetic $La_{0.7}Sr_{0.3}CoO_3$ probed by epitaxial strain, Phys. Rev. Lett. **111**, 257203 (2013).

[5] P. Friš, D. Munzar, O. Caha, and A. Dubroka, Direct observation of double exchange in ferromagnetic $La_{0.7}Sr_{0.3}CoO_3$ by broadband ellipsometry, Phys. Rev. B **97**, 045137 (2018).

[6] J. Fujioka, Y. Yamasaki, H. Nakao, R. Kumai, Y. Murakami, M. Nakamura, M. Kawasaki, and Y. Tokura, Spin-orbital superstructure in strained ferrimagnetic perovskite cobalt oxide, Phys. Rev. Lett. **111**, 027206 (2013).

[7] N. Biškup, J. Salafranca, V. Mehta, M. P. Oxley, Y. Suzuki, S. J. Pennycook, S. T. Pantelides, and M. Varela, Insulating ferromagnetic $LaCoO_{3-\delta}$ films: A phase induced by ordering of oxygen vacancies, Phys. Rev. Lett. **112**, 087202 (2014).

[8] V. V. Mehta, N. Biskup, C. Jenkins, E. Arenholz, M. Varela, and Y. Suzuki, Long-range ferromagnetic order in $LaCoO_{3-\delta}$ epitaxial films due to the interplay of epitaxial strain and oxygen vacancy ordering, Phys. Rev. B **91**, 144418 (2015).

[9] Q. Feng, D. Meng, H. Zhou, G. Liang, Z. Cui, H. Huang, J. Wang, J. Guo, C. Ma, X. Zhai *et al.*, Direct imaging revealing halved ferromagnetism in tensile-strained $LaCoO_3$ thin films, Phys. Rev. Mater. **3**, 074406 (2019).

[10] A. Sotnikov, K.-H. Ahn, and J. Kuneš, Ferromagnetism of $LaCoO_3$ films, SciPost Phys. **8**, 082 (2020).

[11] F. M. F. de Groot, J. C. Fuggle, B. T. Thole, and G. A. Sawatzky, 2*p* x-ray absorption of 3*d* transition-metal compounds—An atomic multiplet description including the crystal-field, Phys. Rev. B **42**, 5459 (1990).

[12] M. A. Korotin, S. Y. Ezhov, I. V. Solovyev, V. I. Anisimov, D. I. Khomskii, and G. A. Sawatzky, Intermediate-spin state and properties of $LaCoO_3$, Phys. Rev. B **54**, 5309 (1996).

[13] C. Zobel, M. Kriener, D. Bruns, J. Baier, M. Gruninger, T. Lorenz, P. Reutler, and A. Revcolevschi, Evidence for a low-spin to intermediate-spin state transition in $LaCoO_3$, Phys. Rev. B **66**, 020402(R) (2002).

[14] A. Ishikawa, J. Nohara, and S. Sugai, Raman study of the orbital-phonon coupling in $LaCoO_3$, Phys. Rev. Lett. **93**, 136401 (2004).

[15] J. Q. Yan, J. S. Zhou, and J. B. Goodenough, Bond-length fluctuations and the spin-state transition in $LCoO_3$ (L = La, Pr, and Nd), Phys. Rev. B **69**, 134409 (2004).

[16] M. W. Haverkort, Z. Hu, J. C. Cezar, T. Burnus, H. Hartmann, M. Reuther, C. Zobel, T. Lorenz, A. Tanaka, N. B. Brookes *et al.*, Spin state transition in $LaCoO_3$ studied using soft x-ray absorption spectroscopy and magnetic circular dichroism, Phys. Rev. Lett. **97**, 176405 (2006).

[17] Z. Ropka and R. J. Radwanski, ^5D term origin of the excited triplet in $LaCoO_3$, Phys. Rev. B **67**, 172401 (2003).

[18] A. Podlesnyak, S. Streule, J. Mesot, M. Medarde, E. Pomjakushina, K. Conder, A. Tanaka, M. W. Haverkort, and D. I. Khomskii, Spin-state transition in $LaCoO_3$: Direct neutron spectroscopic evidence of excited magnetic states, Phys. Rev. Lett. **97**, 247208 (2006).

[19] M. Merz, P. Nagel, C. Pinta, A. Samartsev, H. v. Löhneysen, M. Wissinger, S. Uebe, A. Assmann, D. Fuchs, and S. Schuppler, X-ray absorption and magnetic circular dichroism of $LaCoO_3$, $La_{0.7}Ce_{0.3}CoO_3$, and $La_{0.7}Sr_{0.3}CoO_3$ films: Evidence for cobalt-valence-dependent magnetism, Phys. Rev. B **82**, 174416 (2010).

[20] V. Křápek, P. Novák, J. Kuneš, D. Novoselov, D. M. Korotin, and V. I. Anisimov, Spin state transition and covalent bonding in $LaCoO_3$, Phys. Rev. B **86**, 195104 (2012).

[21] A. Sotnikov and J. Kuneš, Field-induced exciton condensation in $LaCoO_3$, Sci. Rep. **6**, 30510 (2016).

[22] R.-P. Wang, A. Hariki, A. Sotnikov, F. Frati, J. Okamoto, H.-Y. Huang, A. Singh, D.-J. Huang, K. Tomiyasu, C.-H. Du *et al.*, Excitonic dispersion of the intermediate spin state in $LaCoO_3$ revealed by resonant inelastic x-ray scattering, Phys. Rev. B **98**, 035149 (2018).

[23] A. Hariki, R.-P. Wang, A. Sotnikov, K. Tomiyasu, D. Betto, N. B. Brookes, Y. Uemura, M. Ghiasi, F. M. F. de Groot, and J. Kuneš, Damping of spinful excitons in $LaCoO_3$ by thermal fluctuations: Theory and experiment, Phys. Rev. B **101**, 245162 (2020).

[24] D. Fuchs, E. Arac, C. Pinta, S. Schuppler, R. Schneider, and H. v. Loehneysen, Tuning the magnetic properties of $LaCoO_3$ thin films by epitaxial strain, Phys. Rev. B **77**, 014434 (2008).

[25] A. Herklotz, A. D. Rata, L. Schultz, and K. Dorr, Reversible strain effect on the magnetization of $LaCoO_3$ films, Phys. Rev. B **79**, 092409 (2009).

[26] V. V. Mehta, M. Liberati, F. J. Wong, R. V. Chopdekar, E. Arenholz, and Y. Suzuki, Ferromagnetism in tetragonally distorted $LaCoO_3$ thin films, J. Appl. Phys. **105**, 07E503 (2009).

[27] A. D. Rata, A. Herklotz, L. Schultz, and K. Dorr, Lattice structure and magnetization of $LaCoO_3$ thin films, Eur. Phys. J. B **76**, 215 (2010).

[28] W. S. Choi, J.-H. Kwon, H. Jeen, J. E. Hamann-Borrero, A. Radi, S. Macke, R. Sutarto, F. He, G. A. Sawatzky, V. Hinkov *et al.*, Strain-induced spin states in atomically ordered cobaltites, Nano Lett. **12**, 4966 (2012).

[29] D. N. Basov, R. D. Averitt, D. van der Marel, M. Dressel, and K. Haule, Electrodynamics of correlated electron materials, Rev. Mod. Phys. **83**, 471 (2011).

[30] By Alineason Materials Technology GmbH, Germany.

[31] *Handbook of Ellipsometry*, edited by H. G. Tompkins and E. A. Irene (William Andrew, Inc., Norwich, 2005).

[32] P. Augustinský, V. Křápek, and J. Kuneš, Doping induced spin state transition in $LaCoO_3$: Dynamical mean-field study, Phys. Rev. Lett. **110**, 267204 (2013).

[33] M. Dressel and G. Grüner, *Electrodynamics of Solids* (Cambridge University Press, Cambridge, 2002).

[34] M. Zahradník, M. Kiaba, S. Espinoza, M. Rebarz, J. Andreasson, O. Caha, F. Abadizaman, D. Munzar, and A. Dubroka, Photoinduced insulator-to-metal transition and coherent acoustic phonon propagation in $LaCoO_3$ thin films explored by femtosecond pump-probe ellipsometry, Phys. Rev. B **105**, 235113 (2022).

[35] P. F. Maldague, Optical-spectrum of a Hubbard chain, Phys. Rev. B **16**, 2437 (1977).

[36] D. Baeriswyl, C. Gros, and T. Rice, Landau parameters of almost-localized Fermi liquids, Phys. Rev. B **35**, 8391 (1987).

[37] J. Hirsch, Apparent violation of the conductivity sum-rule in certain superconductors, Physica C: Supercond. **199**, 305 (1992).

[38] E. Dagotto, Correlated electrons in high-temperature superconductors, Rev. Mod. Phys. **66**, 763 (1994).

[39] N. N. Kovaleva, A. V. Boris, C. Bernhard, A. Kulakov, A. Pimenov, A. M. Balbashov, G. Khaliullin, and B. Keimer, Spin-controlled Mott-Hubbard bands in $LaMnO_3$ probed by optical ellipsometry, Phys. Rev. Lett. **93**, 147204 (2004).

[40] G. Khaliullin, P. Horsch, and A. M. Oles, Theory of optical spectral weights in Mott insulators with orbital degrees of freedom, Phys. Rev. B **70**, 195103 (2004).

[41] K. Tobe, T. Kimura, Y. Okimoto, and Y. Tokura, Anisotropic optical spectra in a detwinned $LaMnO_3$ crystal, Phys. Rev. B **64**, 184421 (2001).

[42] S. Miyasaka, Y. Okimoto, and Y. Tokura, Anisotropy of Mott-Hubbard gap transitions due to spin and orbital ordering in $LaVO_3$ and YVO_3, J. Phys. Soc. Jpn. **71**, 2086 (2002).

[43] J. Lee, Y. Lee, T. Noh, S. Oh, J. Yu, S. Nakatsuji, H. Fukazawa, and Y. Maeno, Electron and orbital correlations in $Ca_{2-x}Sr_xRuO_4$ probed by optical spectroscopy, Phys. Rev. Lett. **89**, 257402 (2002).

[44] A. Chattopadhyay, A. Millis, and S. Das Sarma, Optical spectral weights and the ferromagnetic transition temperature of colossal-magnetoresistance manganites: Relevance of double exchange to real materials, Phys. Rev. B **61**, 10738 (2000).